

Results from the High Resolution Fly's Eye Experiment

C. C. H. Jui for the High Resolution Fly's Eye Collaboration

Department of Physics, University of Utah, 115 S. 1400 E. Rm. 201 Salt Lake City, Utah, 84112-0830, U.S.A.

Abstract. The High Resolution Fly's Eye (HiRes) Experiment operated two fluorescence detector sites in the western Utah desert between 1997 and 2006. The HiRes results on the cosmic ray spectrum are consistent with the GZK Suppression predicted at $10^{19.8}$ eV and observe an ankle structure at $10^{18.5}$ eV. These spectral features are consistent with a proton-dominated composition for cosmic rays at the highest energies. The HiRes composition studies of both the mean and the variance of the shower maximum depth (X_{max}) also give results that are completely consistent with a predominately protonic composition, and inconsistent with heavy nuclei such as iron. We also report on the result of anisotropy studies.

Keywords: UHECR, cosmic ray, energy spectrum, composition, anisotropy, HiRes

PACS: 98.70.Sa

INTRODUCTION

The High Resolution Fly's Eye experiment made observations of the highest energy cosmic rays between 1997 and 2006. Its two fluorescence detector sites were located on the U.S. Army Dugway Proving Ground in Utah. The HiRes project was a collaboration consisting of the University of Utah, Columbia University, Rutgers University, University of New Mexico, University of Montana, the Los Alamos National Laboratory (LANL), University of Tokyo, and the Institute for High Energy Physics (IHEP) in Beijing, China. The two detector sites were placed on hilltops 12.6 km apart. The HiRes-1 site comprises 22 telescopes covering $3^\circ - 17^\circ$ in elevation, and began monocular observation in 1997. The HiRes-2 site, with 42 mirrors, was added in 2000. This second detector consists of 42 mirrors which view elevation angles in the range $3^\circ - 31^\circ$.

The 64 HiRes telescopes employ the same basic optical design. Ultra-violet (*fluorescence*) photons, emitted in the wake of extensive air showers, are collected using a ~ 2 m diameter spherical mirror (3.7 m² effective collection area) onto a camera of 16×16 pixels at the focal plane. Each pixel consists of a photo-multiplier tube (PMT) and accompanying readout electronics. Each PMT pixel covers a 1° cone in the sky. Each telescope covers about 16° in azimuth and 14° in elevation. In the following sections, we give a brief overview of the results from the HiRes experiment, divided into three major areas: (a) energy spectrum, (b) composition, and (c) arrival anisotropy of ultrahigh energy cosmic rays.

ENERGY SPECTRUM

The HiRes detector design and site separations were optimized to measure cosmic rays at energies $> 10^{18}$ eV.

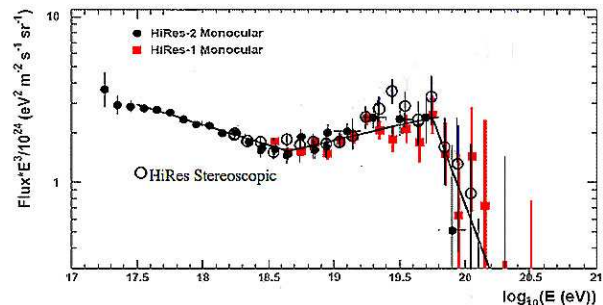


FIGURE 1. Final HiRes energy spectra. The HiRes-1 and HiRes-2 monocular spectra are shown by the red squares and black circles, respectively. The stereo spectrum is shown by the open circles. The GZK cut-off and the ankle features are clearly seen in the data.

The joint HiRes-1 and HiRes-2 monocular spectrum was originally published in 2004 [1]. Figure 1 shows the final monocular [2] and stereo spectra [3] from HiRes. The data clearly shows the Greisen-Zatsepin-Kuz'min cut-off [4] at the expected energy of $10^{19.8}$ eV. A hardening of the spectrum, known as the ankle or *dip* is clearly seen at about $10^{18.6}$ eV as well.

Figure 2 shows the result of fitting the monocular spectra to piece-wise power law models. When only a single continuous power law is assumed (not shown), a chi-squared per degree of freedom ($\chi^2/\text{d.o.f}$) of 162/39 is obtained. With two power laws with a single floating break point, we obtained improved $\chi^2/\text{d.o.f}$ of 63.0/37, where the single break point is found at $10^{18.63}$ eV. Finally, three power laws and two floating breaks gave a $\chi^2/\text{d.o.f}$ of 35.1/35, and break points at $\log_{10} E = 18.65 \pm 0.05$ and 19.75 ± 0.04 . The comparisons of the three $\chi^2/\text{d.o.f}$ figures definitely favor the last model with two breaks, corresponding to an ankle and the GZK cut-off. Moreover, The extrapolation of the power law fit

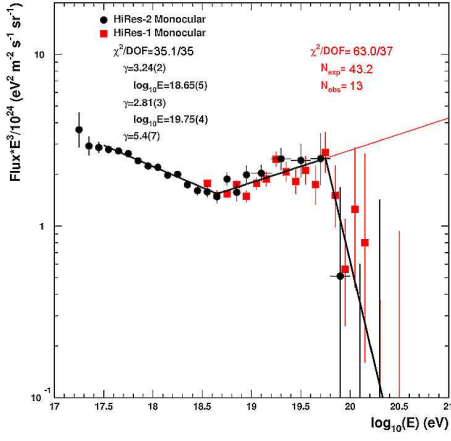


FIGURE 2. Results of fitting the joint HiRes monocular spectrum to piece-wise power laws. The model with two break points (ankle + cut-off) clearly gives a better fit ($\chi^2/\text{d.o.f.}=35.1/35$) than the single break-point model (ankle only)

between the two breaks to higher energies predicts 43.2 events above the second break, whereas only 13 events were observed. The probability for the observed deficit is about 7×10^{-8} , which corresponds to a 5.3σ significance for the observation of the GZK cut-off.

A more theoretically robust estimate of the location of the cut-off was suggested by Berezhinsky *et.al.* [5]. Using the energy $E_{1/2}$ where the integral spectrum falls below half that of the extrapolation of a power law, they obtained $\log_{10} E_{1/2} = 19.72$ for a variety of input source spectral slopes. Figure 3 shows the fit for $E_{1/2}$ from the HiRes data, from which we obtained $\log_{10} E_{1/2} = 19.73 \pm 0.07$. Both this value and the fitted second break point are clearly in excellent agreement with the predicted value of 19.72.

COMPOSITION

Berezhinsky *et.al.* [5] also pointed out that the combination of the observed GZK cut-off and the ankle is a signature of proton-dominated composition at the highest energies. Aloisio *et.al.* [6] also indicated that the shape of the spectrum with these features are essentially model-independent for proton primaries: no fine-tuning is required. The inference of proton dominance is reinforced by the composition studies performed on the HiRes stereo data. The following paragraphs will summarize these studies.

The energy measurement used to compile the spectra depend primarily on the well-established physics associated with electromagnetic showers, and is essentially model-independent. The interpretation of the shower

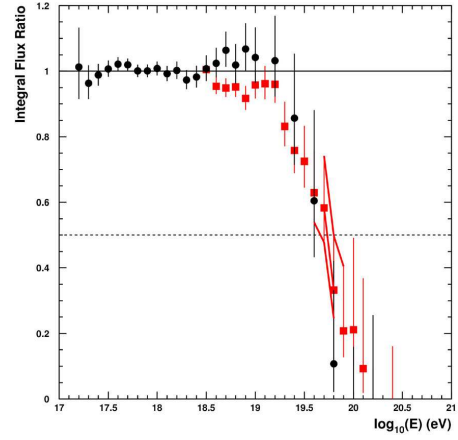


FIGURE 3. Integral spectrum from HiRes monocular data. The HiRes-1 and HiRes-2 points are shown as squares and circles, respectively. From the plot, we obtain $\log_{10} E_{1/2} = 19.73 \pm 0.07$, in good agreement with the robust predictions of Berezhinsky *et.al.* [5].

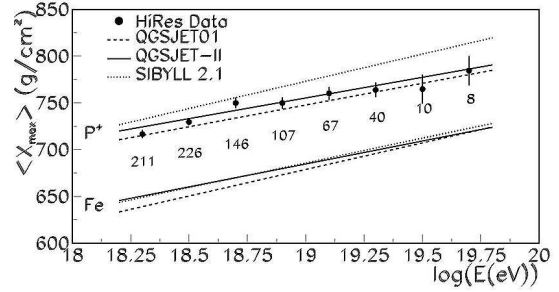


FIGURE 4. Average shower maximum depth ($\langle X_{max} \rangle$) vs. $\log_{10} E$ from HiRes stereo data. For comparison, the predictions are shown for QGSJET01, QGSJET-II, and SIBYLL protons and iron, with full detector simulation. The number of HiRes events in each energy bin is displayed below the data point.

maximum depth, or X_{max} , results rely on comparisons to the predictions of hadronic shower simulations. For this purpose, the HiRes results were compared to CORSIKA [7] generated showers with QGSJET-I [8], QGSJET-II [9] and SYBILL 2.1 [10] hadronic models. Figure 4 shows the average X_{max} values plotted against $\log_{10} E$. The HiRes data is shown by the points [11], and the lines show linear fits to the three hadronic models indicated above for both proton and iron primaries.

On average, the shower maxima are expected to occur deeper into the atmosphere for protons than for iron because of the smaller interaction cross-section as well as lower multiplicity of secondaries for the first interaction of protons compared to iron. For the full range of energies studied, the HiRes data shows an elongation rate, $d \langle X_{max} \rangle / d \log_{10} E$, of $47.9 \pm 6.0(\text{stat.}) \pm 3.2(\text{sys.})$

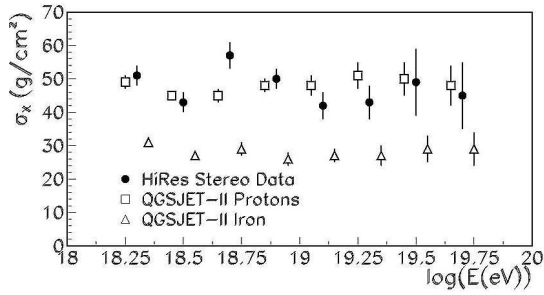


FIGURE 5. X_{max} distribution width vs. $\log_{10}E$ for HiRes stereo data (black points). Expectations from QGSJET-II proton (squares) and iron (triangles) simulations are shown for comparison. The simulation points are shown with small offsets in energy to provide separation.

which is consistent with an unchanging composition. The values $\langle X_{max} \rangle$ in Figure 4 clearly prefer proton primaries over iron. The proton line for the two QGSJET models give excellent description of the HiRes data points. In particular, the QGSJET-II proton line gives a $\chi^2/\text{d.o.f}$ of 6.9/8.

An orthogonal measure of composition is given by the breadth of the X_{max} distributions at a given energy. The smaller interaction cross-section of protons also implies greater fluctuations in the shower maximum for protons than for iron. This simple prediction is supported by CORSIKA simulation, as shown in Figure 5. The QGSJET-II proton and iron predictions for the width are shown with open squares and triangles, respectively. The HiRes stereo data points are shown with black circles, which are clearly consistent with the proton predictions and incompatible with iron.

Figures 4 and 5 used the same HiRes stereo data set. The energy and X_{max} values for each event has also been made available to the public in a data supplement document [12]. This document also contains figures showing the actual X_{max} distributions for HiRes stereo data divided into 0.2 wide $\log_{10}E$ bins, overlaid to QGSJET-II proton or iron distributions. In each case the distributions are completely consistent with the proton model and inconsistent with iron. We show in Figure 6 the overall X_{max} distribution from HiRes data overlaid separately with QGSJET-II proton and iron. These plots again clearly show consistency with the proton model and inconsistency with iron.

ANISOTROPY

HiRes anisotropy searches before 2007 have yielded at best marginal signals (see, for example, reference [13] for report of correlations with BL-Lac objects.) More recent studies with HiRes data have concentrated on two

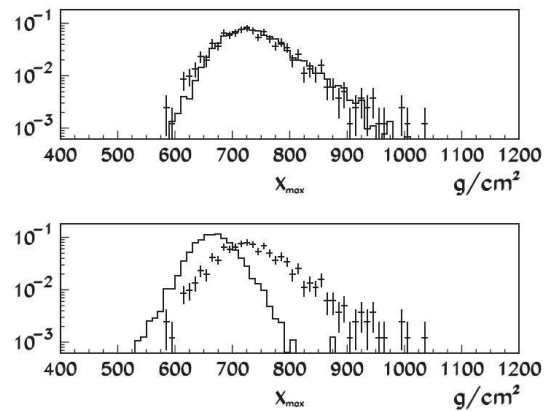


FIGURE 6. Top: X_{max} overlay of HiRes data (points) with QGSJET-II proton Monte Carlo air showers after full detector simulation. Bottom: X_{max} overlay of HiRes data (points) with QGSJET-II iron Monte Carlo air showers.

topics. The first of these is to search for positive correlations with AGNs as reported by the Pierre Auger Observatory (PAO) Collaboration [14]. The corresponding search using the HiRes stereo data with the *a priori* PAO criteria of $(E_{min}, \theta, z_{max}) = (57 \text{ EeV}, 3.1, 0.018)$ yielded only two correlated pairs out of 13 events (comparable in statistics to the original PAO publication [14]) [15]. The number of chance pairings expected was 3.2. The HiRes result, therefore, is completely consistent with isotropy, and inconsistent with the original PAO claim of 8 pairings out of 13 events [14]. Searching within the HiRes data itself also failed to yield any significant correlation with AGNs in the northern sky [15].

A second topic of interest is to look for a correlation of arrival directions with the large scale structure (LSS) in the nearby universe. The local LSS model used is based on the 2 Micron All-Sky Redshift Survey (2MRS) [16]. The galactic plane (galactic latitude $|b| < 10^\circ$) and objects within 5 Mpc are removed, and an isotropic distribution is assumed beyond 250 Mpc. The magnetic bending is simulated using (variable) Gaussian smearing.

In carrying out this study [17], many event sets equivalent to HiRes exposure are generated according to either the LSS model, or a completely isotropic source distribution. These sets varied in the lower energy cut-off and in the (magnetic) Gaussian smearing. The average over many sets for each pair of threshold energy and smearing angle is then compared to the actual data distribution using a Kolmogorov-Smirnov test. Figure 7 shows an example of these comparisons for the case of the LSS model, $E_{min} = 4.0 \times 10^{19} \text{ eV}$, and 6° smearing.

The final results of this study are shown in figure 8. The HiRes data was completely consistent with isotropic source distributions for (*a priori*) threshold energies of 10, 40 and 57 EeV and for all smearing angles up to 15° .

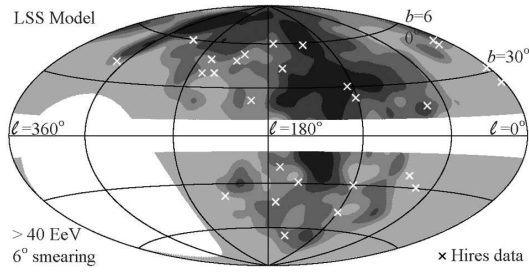


FIGURE 7. Hammer projection in galactic coordinates of LSS simulated event density with threshold of 40 EeV and 6° smearing. The bands show areas of equal number of events; the darker bands show higher density. HiRes events are shown with the "x" symbols.

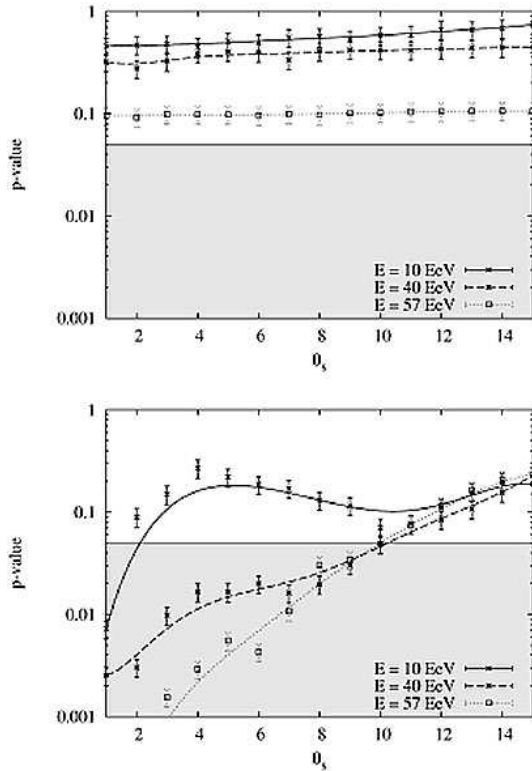


FIGURE 8. Plots of K-S test p values for HiRes data against isotropic source model (top) and the LSS model (bottom) for threshold energies of 10, 40 and 57 EeV and smearing angles up to 15°

The data also show poor agreement with the LSS model, and exclude correlation at 95% c.l. for $E > 40$ EeV and smearing angles less than 10° . The HiRes stereo data set used in the recent anisotropy studies along with exposure calculations have been made available to the public [18].

ACKNOWLEDGMENTS

This work is supported by the National Science Foundation under contracts NSF-PHY-9321949, NSF-PHY-9322298, NSF-PHY-9974537, NSF-PHY-0071069, NSF-PHY-0098826, NSF-PHY-0140688, NSF-PHY-0245328, NSF-PHY-0307098, and NSF-PHY-0305516, by Department of Energy grant FG03-92ER40732, by the BSP under IUAP VI/11, by the FNRS contract 1.5.335.08 and by the IISN contract 4.4509.10. We gratefully acknowledge the contribution from the technical staffs of our home institutions and thank the University of Utah Center for High Performance Computing for their contributions. The cooperation of Colonels E. Fisher, G. Harter, and G. Olsen, the US Army and the Dugway Proving Ground staff is appreciated.

REFERENCES

1. R. U. Abbasi *et al.* (HiRes Collaboration), (astro-ph/0208243) Phys.Rev.Lett. **92**, 151101 (2004).
2. R. U. Abbasi *et al.* (HiRes Collaboration), Phys. Rev. Lett. **100**, 101101 (2008) (astro-ph/0703099v2).
3. R. U. Abbasi *et al.* (HiRes Collaboration), Measurement of the (arXiv:0904.4500[astro-ph]) Astropart.Phys. **32**, 53 (2009).
4. K. Greisen, Phys. Rev. Lett. **16**, 748 (1966); G.T. Zatsepin and V.A. Kuz'min, Pis'ma Zh. Eksp. Teor. Fiz. **4**, 114 (1966) [JETP Lett. **4**, 78 (1966)].
5. Berezhinsky, Gazizov, and Grigorieva, Phys. Rev. D **74**, 043005 (2006).
6. R. Aloisio *et al.*, Astropart. Phys. **27** 76 (2007).
7. D. Heck *et al.*, Forschungszentrum Karlsruhe Tech. Rep. FZKA 6019, 1998; D. Heck *et al.*, Forschungszentrum Karlsruhe Tech. Rep. 2001.
8. N. N. Kalmykov and S. S. Ostapchenko, Phys. At. Nucl. **56**, 346 (1993).
9. S. Ostapchenko, Nucl. Phys. B, Proc. Suppl. **151**, 143 (2006).
10. R. Fletcher *et al.*, Phys. Rev. D **50**, 5710 (1994); R. Engel *et al.*, in Proc. 26th Intl. Cosmic Ray Conference, Salt Lake City, Utah, 1999 (University of Utah, Salt Lake City, Utah, 1999).
11. R. U. Abbasi *et al.* (HiRes Collaboration), Phys. Rev. Lett. **104**, 161101 (2010).
12. Data supplement to Phys. Rev. Lett. **104**, 161101 (2010); found at <http://www.cosmic-ray.org/journals/prl.html>
13. R. U. Abbasi *et al.*, Astrophys. Journal **636**, 680 (2006)
14. Abrahams *et al.*, Science **318**, 938 (2007).
15. R. U. Abbasi *et al.* (HiRes Collaboration), (arXiv:0804.0382 [astro-ph]) Astroparticle Physics **30**, 175 (2008).
16. J. Huchra *et al.* (2010), in preparation.
17. R. U. Abbasi *et al.* (HiRes Collaboration), Astrophys. J. Lett. **713** L64-L68 (2010).
18. <http://www.cosmic-ray.org/supplements.html>

Copyright of AIP Conference Proceedings is the property of American Institute of Physics and its content may not be copied or emailed to multiple sites or posted to a listserv without the copyright holder's express written permission. However, users may print, download, or email articles for individual use.